

Interpretation of non-linear chemical shifts in XPS/AES features in non-crystalline zirconium silicate alloys: $(\text{ZrO}_2)_x(\text{SiO}_2)_{1-x}$

G.B. Rayner, Jr., D. Kang, and G. Lucovsky
 Depart. of Physics, NC State Univ., Raleigh, NC 27695

Based on systematic shifts in binding energies that derive from different near-neighbor bonding of transition metal (TM) and Si-atoms, X-ray photoelectron spectroscopy (XPS) has been used to distinguish TM oxide and silicate alloy bonding arrangements. This paper presents new XPS and Auger electron spectroscopy (AES) results for Zr silicate alloys prepared by plasma processing. The compositional dependencies of XPS binding energies and AES kinetic energies are compared with Zr-, Si- and O-atom partial charges calculated from a self-consistent empirical chemical bonding model previously applied to ir-active vibrations of Si-H groups in Si suboxide alloys. Non-crystalline Zr silicate alloys $((\text{ZrO}_2)_x(\text{SiO}_2)_{1-x})$ present an interesting test for this approach, primarily because of a chemically-ordered compound phase (ZrSiO_4) at $x = 0.5$. Based on ir results, $x = 0.5$ separates non-crystalline alloy compositions into two qualitatively different bonding regimes. For $x < 0.5$, the local bonding components are Zr ions, and a *disrupted* SiO_2 continuous random network in which the number of terminal and bridging O-atoms bonded to a given Si-atom is determined by random bonding statistics. Between $x = 0.5$ and 1.0, bonding is primarily ionic with: i) positive Zr^{4+} , and negative ii) silicate (SiO_4^{4-}) and iii) O^{2-} ions.

Figures 1(a), (b) and (c) indicate binding energies of O 1s, Zr 3d, and Si 2p XPS features as a function of x . The approximately linear behavior of the O 1s feature reflects a chemically-averaged bonding environment consistent with the empirical model, whilst the distinctly non-linear behavior for the Zr 3d and Si 2p features reflects systematic changes as a function of x which are not in accord with the empirical bonding model, and will instead be interpreted in the context of ab initio calculations that include dipolar network atom fields. Figure 2 indicates a non-linear behavior in the Zr_{MNN} AES feature that is complementary to the non-linear dependence in Fig. 1(b). There is also XPS spectroscopic evidence for a chemical phase separation of Zr silicate alloys into ZrO_2 and SiO_2 components after a 900°C rapid thermal anneal. This data complements ir and X-ray diffraction studies that also reveal the chemical phase separation.

The non-linear behavior in Figs. 1(b) and 2 has been correlated with changes in the bonding coordination of Zr atoms in the alloy concentration regime up to about $x = 0.5$, providing additional evidence to support a microscopic bonding model for dielectric constant enhancements that are unique to group IVB silicate alloys. The bonding coordination of Zr increases from four to eight with increasing x as chemical bonds with O-atoms replace network *dipole polarization fields*. In addition, the results in Figs. 1(b) and (c) indicate nearly equal total shifts of ~ 1.8 eV between the Si 2p and Zr 3d binding energies over the entire alloy range. When combined with shifts in valence band offset energies with respect to Si from AES, these predict that conduction band offset energies of Zr silicate alloys will not depend on x , but *quantitative effects* on tunneling current will be alloy dependent, reflecting their localized d-state origin.

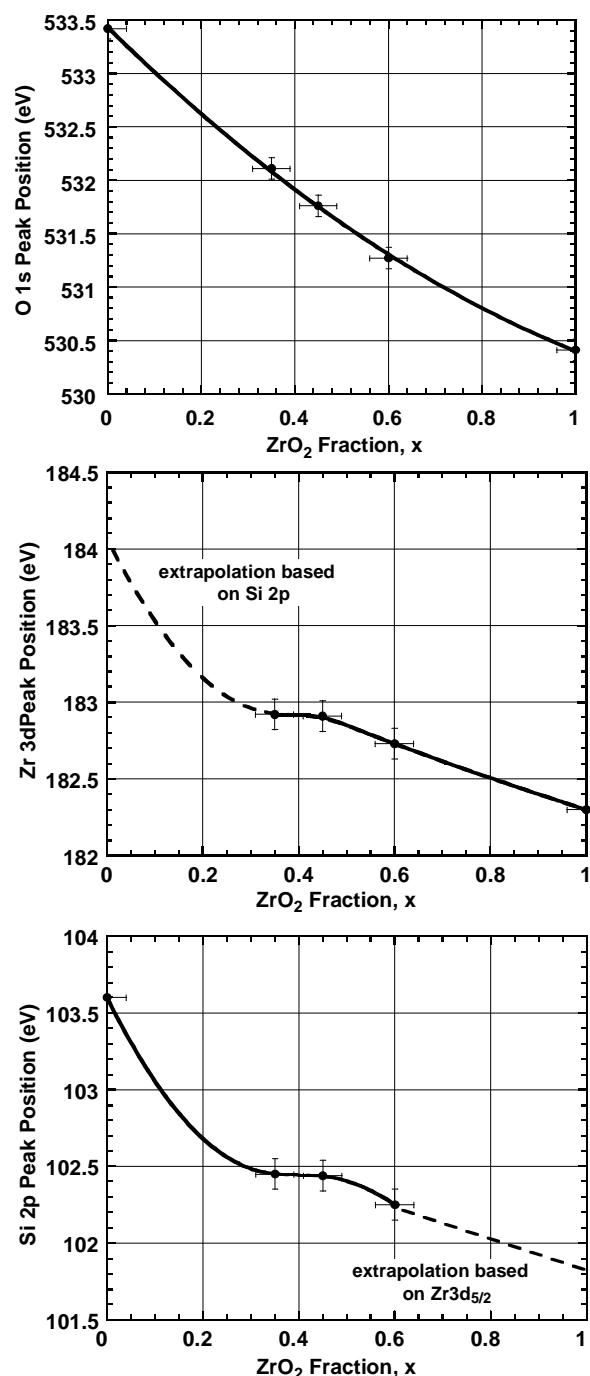


Figure 1. XPS peak positions for (a) O 1s, (b) Zr $3d_{5/2}$, and (c) Si 2p features in Zr silicate alloys subjected to a 500°C , 30 s rapid thermal anneal.

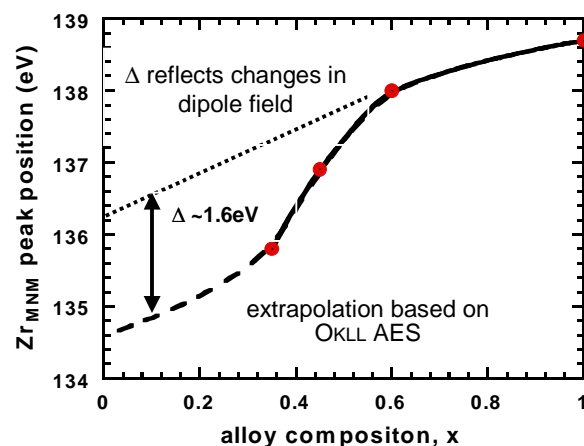


Figure 2. AES kinetic energy for the highest energy Zr_{MNN} feature as a function of alloy composition.